

Magnetic-Field-Induced Normal Force of Magnetorheological Elastomer under Compression Status

Guojiang Liao, Xinglong Gong,* Shouhu Xuan, Chaoyang Guo, and Luhang Zong

CAS Key Laboratory of Mechanical Behavior and Design of Materials, Department of Modern Mechanics, University of Science and Technology of China, Hefei, 230027, China

ABSTRACT: The magnetic-field-induced normal force of magnetorheological elastomer (MRE) under compression status is studied in this paper. The influence of monotonic loading of the magnetic field, particle distribution, temperature, and cyclic loading of the magnetic field are investigated. The experimental results show that the normal force increases with increasing magnetic field and precompression force. For aligned MRE, the change of the magnetic-field-induced normal force is larger than that of isotropic MRE due to the special chainlike structure. When the temperature increases, the maximum change of the magnetic-field-induced normal force first increases and then decreases, due to the interaction of iron particles and the decreasing of the saturation magnetization of the carbonyl iron particles. If the magnetic field is circularly applied on the MRE, the normal force during unloading is smaller than that during loading due to the stress relaxation.

1. INTRODUCTION

Magnetorheological elastomer (MRE) belongs to a kind of intelligent material whose rheological properties are controlled rapidly by varying the externally applied magnetic field.^{1,2} It is the solid analogue of magnetorheological fluid while it overcomes the disadvantages existing in magnetorheological fluid, such as particle settling, environmental contamination, and sealing problems. MRE is usually comprised of rubber or rubberlike material (as the matrix), microsized iron particles (as the fillers), and some other additives.^{3,4} Due to its special rheological properties, MRE has attracted more and more attention in recent years. Ginder et al.⁵ investigated the magnetic-field-induced shear property of MRE. Li et al.⁶ investigated the viscoelastic property of MRE. Kallio et al.⁷ studied the dynamic compression property of MRE. Fan et al.³ investigated the damping property of MRE. To illustrate these magnetic-field-induced rheological properties, many theories also have been proposed. Jolly et al.¹ developed the magnetic dipole theory to explain the shear property of MRE; Davis et al.² introduced the finite element method to study MRE materials; Zhang et al.^{8,9} proposed a Gaussian distribution model based on anisotropic MRE.

In the past decade, most of the research has focused on the magnetic-field-induced shear property of MRE.^{1,2,5,6,8–19} Based on this shear property, MRE can be applied in vibration absorbers, vibration isolators, engineering mounts and bushings, etc.^{4,14–20} Polymer-based materials can bear more loads in compression status than in shear status, and most of them often work in compression status. Thus the mechanical property under compression status is very important for a polymer and its composite materials.^{21,22} To this end, the mechanical property of MRE under compression status also should be investigated so as to evaluate its practical applications. Kaillo studied the changes in the stiffness and vibration damping of MRE under the influence of a magnetic field when tested in dynamic compression.⁷ Koo investigated the dynamic compression properties of MRE under cyclic loading and proposed a phenomenon model

to explain the experimental results.²³ Bica studied the compressibility modulus using the flat MRE-capacitor method.²⁴ These researchers did enlightening studies on the compression property of magnetorheological elastomer. Clearly, the understanding of the compression property is beneficial to enlarging the application of magnetorheological elastomer. In addition, MREs show a special magnetostrictive characteristic, which enables them much potential in sensors, actuators, etc.^{25–27} When an external magnetic field is applied, the elongation of MRE is quite large. As a potential magnetostriction material, its normal force under compression status is unique for its practical application.^{28,29} Therefore, more work should be done to thoroughly investigate the normal force of the MRE under fixed strain.

In this work, the normal force of MRE under compression status is studied both experimentally and theoretically. MRE is first synthesized by using silicone rubber as the matrix, and its normal force is evaluated by using a rheometer. The influence of the loading type of the magnetic field, particle distribution, and temperature are investigated in detail. A modified magnetic dipole theory is proposed to illustrate the property of normal force. This work presents the normal force of MRE coupled with the magnetostrictive process, and they are very useful in designing actuators, sensors, etc.^{28,29}

2. EXPERIMENTAL DETAILS

2.1. Sample Preparation. The materials of fabricated MRE samples consist of carbonyl iron particles (type CN, with average diameter 6 μm , provided by BASF Co., Germany), HTV silicone rubber (type MVQ 110-2, from Dong Jue Fine Chemicals Nanjing Co. Ltd.), di(2-ethylhexyl) phthalate (from Shanghai Resin Factory Co. Ltd.), and vulcanizing

Received: September 1, 2011

Revised: November 26, 2011

Accepted: January 30, 2012

Published: January 30, 2012

agent (double methyl double benzoyl hexane, from Shenzhen Gujia Co.). Di(2-ethylhexyl) phthalate was used as plasticizer to improve the process of rubber mixing and to adjust the initial modulus of MRE. The mass ratio of iron particles to the other materials is 4:1.

Two kinds of MRE samples were fabricated. One was isotropic MRE, and the other was aligned MRE. The procedure of fabricating aligned MRE is as follows: First, the HTV silicone rubber was subjected to heat treatment at 150 °C for 4 h to reduce the air bubbles in the rubber. Then, the rubber was placed in a double-roll mill (Taihu Rubber Machinery Inc., China, Model XK-160) to be thoroughly mixed with iron particles, di(2-ethylhexyl) phthalate, and vulcanizing agent for roughly 1 h. Later, the rubber mixture was used to fabricate MRE samples. The rubber mixture was placed into a mold. Then the mold was fixed to a customized Magnet-Heat coupled device, whose sketch is shown in Figure 1. This device can keep

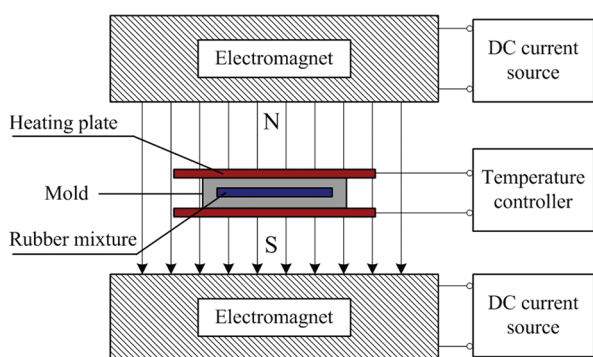


Figure 1. Sketch of customized Magnet-Heat coupled device.

the rubber mixture at a fixed temperature and supply a vertical magnetic field. The temperature in this process was 120 °C, and the magnetic field was roughly 1.5 T. This process was called “prestructure”, and it lasted for 15 min. In the prestructure process, the iron particles in the rubber mixture were aligned along the direction of the magnetic field and the chainlike structures of iron particles were formed. Then the mold with the rubber mixture was placed on a flat vulcanizer (Bolon Precision Testing Machines Co., China, Model BL-6170-B) for vulcanizing. The vulcanizing process was conducted at a temperature of 160 °C for 5 min. After that, the aligned MRE samples were obtained.

For the aligned MRE, the iron particles form chainlike structures in the prestructure process and these chainlike structures are kept during vulcanization. The isotropic MRE is prepared without the prestructure process, no chainlike structures are formed and the iron particles are dispersed uniformly.

2.2. Normal Force Test. The normal force of MRE was tested by using a rheometer (Physica MCR 301, Anton Paar), whose working principle is shown in Figure 2. The testing magnetic field strength was adjusted by controlling the current applied to the electromagnetic coil, and the testing temperature was controlled by a fluid circulator with water. The size of each sample is 10 mm in radius and 1 mm in thickness. The sample was placed under the rotating disk. The process of the normal force test is as follows. First, a precompression force was applied on the MRE sample by the rotating disk. After the precompression force reached the expected value, the position was maintained. Then the normal force was tested under different magnetic flux densities and different temperatures (25, 50, 70, and 90 °C). Each sample was tested three times under the same condition. From the test, the relationship between the precompression force and strain is as shown in Figure 3.

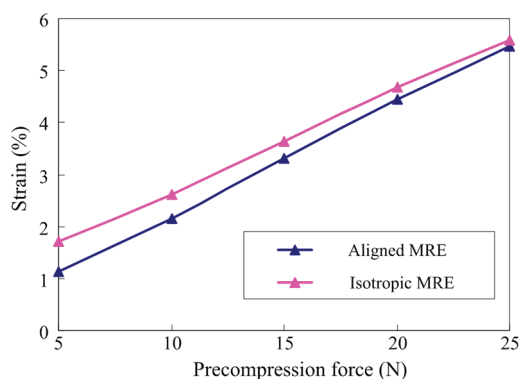


Figure 3. Relationship of precompression force versus strain.

The compression strain is between 1 and 5%, which is proper for rubber materials.

2.3. Characterization of Microstructure. To observe the microstructures of the samples, the samples were cut into pieces and observed by a digital microscope (type VHX-100, KEYENCE).

2.4. Magnetization Test. To investigate the magnetization changes of the iron particles, the magnetization of the particles was measured by a SQUID (Quantum Design Co., America).

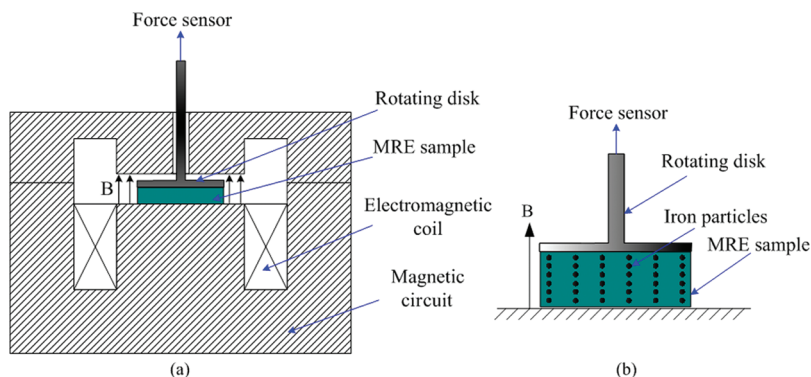


Figure 2. (a) Principle diagram of MR device of rheometer. (b) Arrangement of aligned MRE in the rheometer.

3. RESULTS AND DISCUSSION

3.1. Influence of Monotonic Loading of Magnetic Field on the Normal Force of Aligned MRE. The normal force of aligned MRE under different magnetic flux densities and different precompression forces is shown in Figure 4. It is

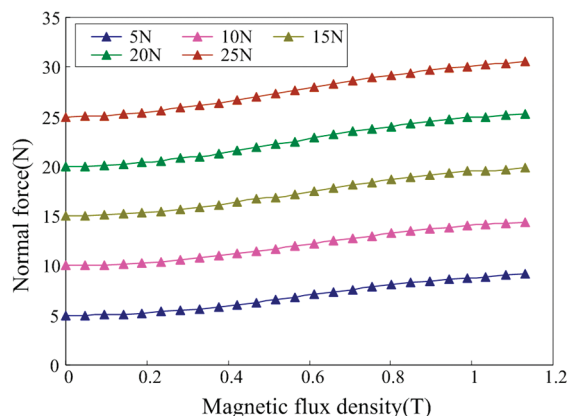


Figure 4. Normal force of aligned MRE under different magnetic flux densities and different precompression forces.

found that the normal force increases with increasing magnetic flux density. When the magnetic flux density increases to 1.1 T, the normal force reaches saturation. The carbonyl iron particles which were used show a soft magnetic property, and their magnetization curve also exhibits a saturation characteristic. Therefore, the change of normal force is resulted from the magnetizing process of iron particles and the magnetic–magnetic interactions between the magnetic particles. In Figure 4, the different data points marked by different colors are obtained by testing the normal force of MRE under different precompression forces. The increasing tendencies of the normal force with the increasing of magnetic flux density are almost the same. However, the maximum changes of normal force are different. As shown in Figure 5, the maximum change of normal force increases with

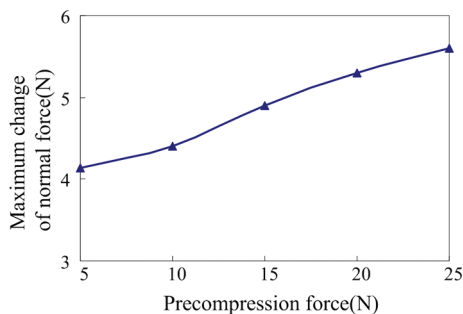


Figure 5. Maximum change of normal force under different precompression forces.

increasing precompression force. For example, when the precompression force is 5 N, the maximum change of normal force is 4.14 N. When the precompression force reaches 25 N, the maximum change of normal force reaches 5.6 N. The change of the normal force results from the interaction of the iron particles. When the precompression force increases, the distance of the adjacent iron particles decreases, and this leads the interaction between the adjacent particles to increase. Therefore, the maximum change of the normal force with large precompression force is larger than that with small precompression force.

The iron particles form chainlike structures in the aligned MRE.^{2,6,8–13,30} On the basis of observation of these chainlike structures, Jolly¹ and Davis² has proposed magnetic dipole theory to investigate the rheological properties of aligned MRE. This theory can successfully illustrate the shear properties of aligned MRE at magnetic saturation status. In this work, on the basis of magnetic dipole theory, a possible theory model was proposed to investigate the normal force of aligned MRE. Figure 6 shows the magnetic dipole model of the aligned MRE.

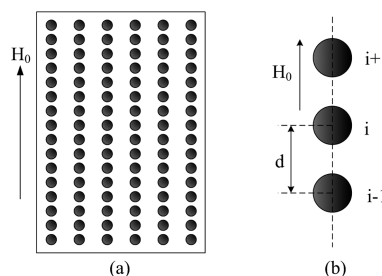


Figure 6. Magnetic dipole model of aligned MRE: (a) MRE with chainlike structures; (b) magnetic dipoles in a single particle chain.

It is assumed that the particles are aligned in long chains, and only the interactions between particles within the chain were considered.¹

Considering the high-field limit and calculating the maximum change in normal force due to the applied magnetic field, all the particles are magnetically saturated. Thus each iron particle has a magnetic dipole moment^{1,2}

$$m = \mu_0 V M_s \quad (1)$$

where μ_0 is the permeability of vacuum, V is the volume of the iron particles, and M_s is the saturation magnetization. The interaction energy of an iron particle marked i and the other particles within a chain is¹

$$E = \frac{-1}{4\pi\mu_m\mu_0} \frac{4\zeta m^2}{d^3} \quad (2)$$

where μ_m is the relative permeability of the rubber matrix, m is the magnetic dipole moment of each iron particle, d is the distance of two adjacent particles, and $\zeta = \sum_{k=1}^{\infty} 1/k^3 \approx 1.202$. Then the total magnetic energy of a MRE sample can be expressed as

$$E_t = \frac{\phi V_t}{2V} E \quad (3)$$

where V_t is the volume of MRE sample and ϕ is the volume fraction of iron particles in the composites. Thus the total magnetic energy density (energy per unit volume) is

$$E_d = \frac{E_t}{V_t} = \frac{\phi}{2V} E \quad (4)$$

The compression strain of the MRE sample can be expressed as

$$\varepsilon = \frac{d - d_0}{d_0} \quad (5)$$

where d is the distance of adjacent particles and d_0 is the initial distance of adjacent particles. The magnetic-field-induced stress can be expressed as^{1,2}

$$\sigma = \frac{\partial E_d}{\partial \epsilon} = \frac{\partial E_d}{\partial d} \frac{\partial d}{\partial \epsilon} = d_0 \frac{\partial E_d}{\partial d} \quad (6)$$

Therefore the magnetic-field-induced compression force is

$$F = \sigma S \quad (7)$$

where S is the compression area of the MRE sample. Substitute eqs 1, 2, 3, 4, and 6 into eq 7, then the magnetic-field-induced normal force can be expressed as

$$F = \frac{3Sd_0\phi_0^2 V \mu_0 M_s^2}{2\mu_m \pi d^4} \quad (8)$$

Equation 8 shows that the maximum magnetic-field-induced normal force is related to two factors: the magnetization and the interparticle distance. The magnetic-field-induced normal force increases with increasing magnetization and decreasing interparticle distance. The distance of the adjacent particles decreases when the precompression force increases. Thus the maximum magnetic-field-induced normal force increases, which agrees well with the experimental results as shown in Figure 5.

3.2. Influence of Particle Distribution on the Normal Force of MRE. Figure 7 shows the normal force of isotropic

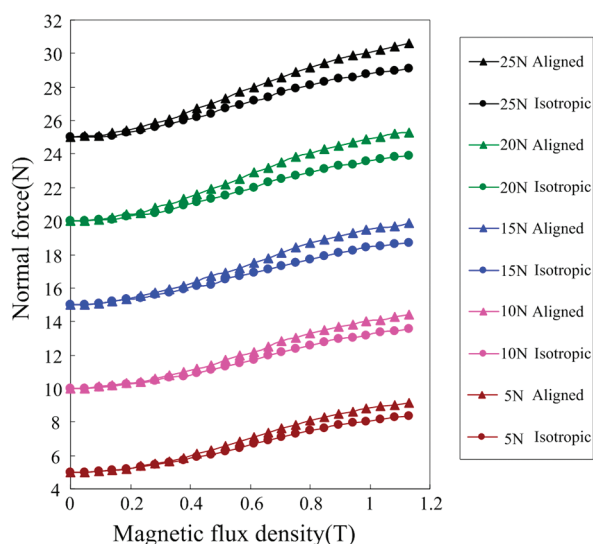


Figure 7. Comparison of normal forces of isotropic MRE and aligned MRE under different precompression forces.

MRE under monotonic loading of the magnetic field. The comparison of isotropic MRE and aligned MRE is also shown in Figure 7. Similar to the aligned MRE, the normal force of the isotropic MRE also increases with increasing magnetic flux density. When the magnetic flux density is around 1.1 T, the normal force is saturated due to the magnetic saturation of iron particles. When the precompression force increases, the maximum change of normal force increases due to the decreasing distance between adjacent particles. Comparing isotropic MRE with aligned MRE, the normal force of the isotropic MRE is smaller than that of aligned MRE under the same conditions. This difference reaches a maximum value when the normal force is saturated.

Figure 8 shows the comparison of the maximum change of normal force of isotropic MRE and aligned MRE. It is found

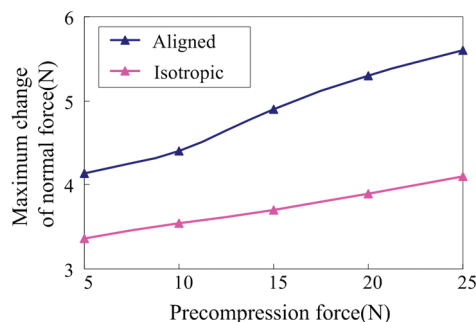


Figure 8. Comparison of maximum changes of magnetic-field-induced normal forces of aligned MRE and isotropic MRE under different precompression forces.

that the maximum changes of normal force of both isotropic MRE and aligned MRE increase with increasing precompression force. However, the change of normal force of aligned MRE is much bigger than that of isotropic MRE, which is mainly due to the different distributions of iron particles. With the same volume fraction of iron particles, the average distance of iron particles in isotropic MRE is much larger than that in aligned MRE.³¹ Figure 9 shows the microstructures of isotropic MRE and aligned MRE, which clearly demonstrate that the distance of adjacent particles of isotropic MRE is much larger than that of aligned MRE. In section 3.1, the magnetic dipole theory is used to illustrate the magnetic-field-induced normal force. The theory is based on the assumption that the magnetic interaction occurs within a chain and it cannot be used to describe the normal force of isotropic MRE. Because the magnetic-field-induced normal force is due to the interaction of the iron particles, the uniform distribution of iron particles makes the distance of adjacent particles much larger for isotropic MRE. Thus the magnetic interaction of iron particles is much smaller for isotropic MRE. This is the main reason why the magnetic-field-induced normal force of isotropic MRE is smaller than that of aligned MRE. Actually, the difference in mechanical properties of aligned MRE and isotropic MRE can also be found in the shear property test for the same reason, which has been proved by many researchers.^{2,6,8-13,30,32-34}

3.3. Influence of Temperature on the Normal Force of MRE. Figure 10 shows the influence of temperature on the normal force of MRE under monotonic loading of magnetic field. Figure 11 shows the magnetization change of the iron particles measured by a SQUID (Quantum Design Co., America). Due to the decreasing particle distance, the maximum change of normal force increases when the precompression force increases. When the temperature increases, the maximum change of the normal force first increases and then decreases. The change of the normal force is due to the interaction of the particles. As shown in eq 8, the magnetic-field-induced normal force is related to the magnetization, M_s . Figure 11 shows that the magnetization of the iron particles decreases with increasing temperature. Therefore, when the temperature increases, the magnetization, M_s , of the iron particles decreases, which leads to the decreasing of the maximum change of the normal force. On the other hand, when the temperature increases, the modulus of the rubber matrix decreases. Thus, when the temperature increases, the rubber matrix becomes softer. A softer matrix benefits the movement of the iron particles.

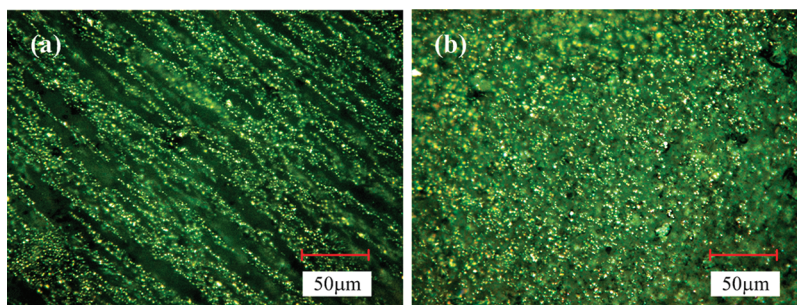


Figure 9. Photographs of (a) aligned MRE and (b) isotropic MRE.

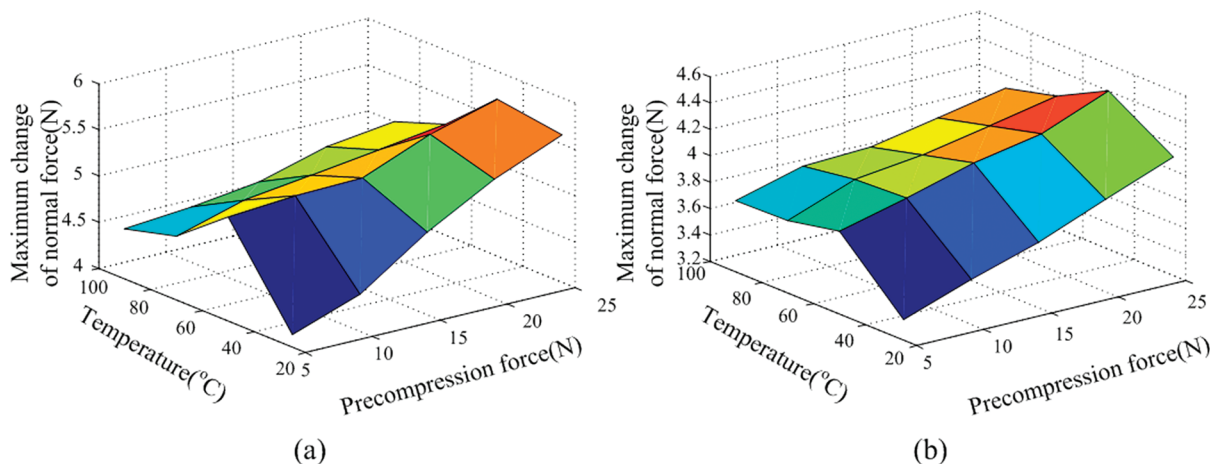


Figure 10. Influence of temperature on normal force of two kinds of MRE under monotonic loading of magnetic field: (a) aligned MRE; (b) isotropic MRE.

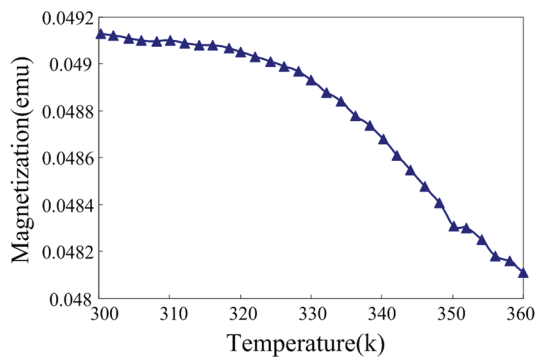


Figure 11. Magnetization change of iron particles.

Therefore, the interaction between the iron particles becomes larger when the temperature increases, ignoring the influence of the magnetization. Larger magnetic interaction between particles leads to larger magnetic-field-induced normal force of the MRE sample. Thus, when the temperature increases, there are two factors that influence the magnetic-field-induced normal force. One is the magnetization, and the other is the modulus of the rubber matrix. The effects of the two factors are opposite. Therefore, when the temperature increases, the maximum change of magnetic-field-induced normal force increases first and decreases later.

3.4. Influence of Cyclic Loading of Magnetic Field on the Normal Force of MRE. The normal force of aligned MRE under cyclic loading was investigated. The magnetic current increased from 0 to 5 A and then decreased to 0 A. After that, the direction of the current was reversed. Then, the current

increased to 5 A and decreased to 0 A. The experimental time lasted 300 s, and 100 data points were collected.

Figure 12 shows the experimental results of magnetic-field-induced normal force of aligned MRE under cyclic loading.

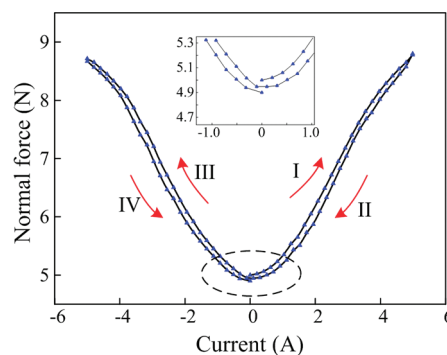


Figure 12. Magnetic-field-induced normal force of aligned MRE under cyclic loading: I, loading; II, unloading; III, reverse loading; IV, reverse unloading.

When the direction of the magnetic field reverses, the magnetic-field-induced normal force shows a tendency similar to that of the normal force when the direction of the magnetic field is unchanged. This indicates that the normal force of MRE is independent of the direction of the magnetic field. In addition, the normal force with increasing magnetic field is not as same as the normal force with decreasing magnetic field. If the magnetic field is the same, the magnetic-field-induced normal force during unloading is smaller than that during loading.

Comparing the normal force before cyclic loading with that after cyclic loading, it is observed that the normal force after cyclic loading is smaller than that before cyclic loading.

To further study the above phenomenon, the influence of cyclic loading of the magnetic field on the normal force of aligned MRE under different precompression forces was investigated. The curves under different precompression forces show similar tendencies (Figure 12). For simplicity, the curves under different precompression forces are not plotted. Instead, the difference in the normal force before cyclic loading and after cyclic loading is plotted in Figure 13. Under different

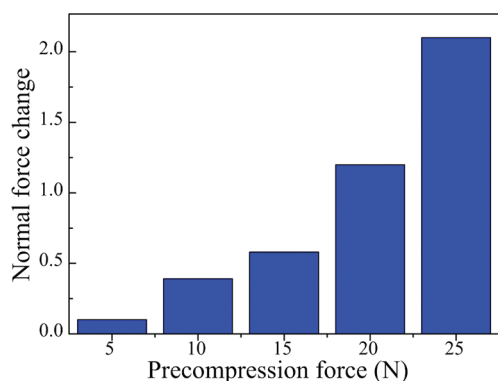


Figure 13. Difference of the normal force before cyclic loading and after cyclic loading.

precompression forces, the normal force after cyclic loading is smaller than that before cyclic loading. In addition, the difference increases with increasing precompression force. This phenomenon may result from the stress relaxation of MRE. Figure 14 shows the experimental results of the stress relaxation

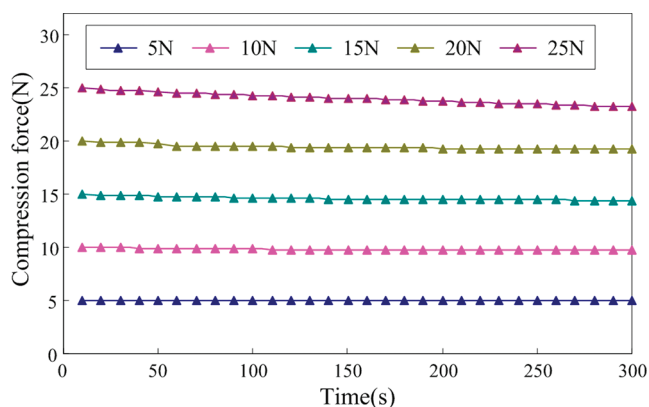


Figure 14. Stress relaxation of aligned MRE under different precompression forces (without magnetic field).

process of aligned MRE under different precompression forces in the absence of a magnetic field. It is found that the speed of stress relaxation increases with increasing precompression force. This agrees well with the results shown in Figure 13. Moreover, the difference in the normal force before cyclic loading and after cyclic loading may also respond to some irreversible change of structure named the Mullins effect.³⁵

4. CONCLUSION

This paper presents the magnetic-field-induced normal force of MRE under compression status. The influence of monotonic

loading of the magnetic field, particle distribution, temperature, and cyclic loading of the magnetic field were investigated. It is found that the magnetic-field-induced normal force increases with increasing magnetic field and increasing precompression force. The interaction of the iron particles increases when the magnetic field and/or the precompression force increases. Thus the magnetic-field-induced normal force increases. For the aligned MRE, the maximum change of magnetic-field-induced normal force is larger than that of isotropic MRE due to the special chainlike structure of iron particles which is formed in the process of prestructure. The saturation magnetization of the carbonyl iron particles decreases and the modulus of the rubber matrix decreases when the testing temperature increases. Therefore, the magnetic-field-induced normal force first increases and then decreases with increasing testing temperature. Besides, the cyclic loading of the magnetic field is applied on MRE to investigate its magnetic-field-induced normal force. It is found that the magnetic-field-induced normal force is not related to the direction of the magnetic field. When the magnetic field is the same, the magnetic-field-induced normal force during unloading is smaller than that during loading. Besides, under different precompression forces, the normal force after cyclic loading is smaller than that before cyclic loading and the difference increases with increasing precompression force.

■ AUTHOR INFORMATION

Corresponding Author

*E-mail: gongxl@ustc.edu.cn.

■ ACKNOWLEDGMENTS

Financial support from the National Natural Science Foundation of China (Grants 11125210, 11072234, 11102202), the Specialized Research Fund for the Doctoral Program of Higher Education of China (Project No. 20093402110010), and the Fundamental Research Funds for the Central Universities (No. WK2090000002) is gratefully acknowledged.

■ REFERENCES

- (1) Jolly, M. R.; Carlson, J. D.; Munoz, B. C. A model of the behaviour of magnetorheological materials. *Smart Mater. Struct.* **1996**, *5*, 607.
- (2) Davis, L. C. Model of magnetorheological elastomers. *J. Appl. Phys.* **1999**, *85*, 3348.
- (3) Fan, Y. C.; Gong, X. L.; Jiang, W. Q.; Zhang, W.; Wei, B.; Li, W. H. Effect of maleic anhydride on the damping property of magnetorheological elastomers. *Smart Mater. Struct.* **2010**, *19*, No. 055015.
- (4) Liao, G. J.; Gong, X. L.; Kang, C. J.; Xuan, S. H. The design of an active-adaptive tuned vibration absorber based on magnetorheological elastomer and its vibration attenuation performance. *Smart Mater. Struct.* **2011**, *20*, No. 075015.
- (5) Ginder, J. M.; Nichols, M. E.; Elie, L. D.; Tardiff, J. L. Magnetorheological elastomers: Properties and applications. *Proc. SPIE* **1999**, *3675*, 131.
- (6) Li, W. H.; Zhou, Y.; Tian, T. F. Viscoelastic properties of MR elastomers under harmonic loading. *Rheol. Acta* **2010**, *49*, 733.
- (7) Kallio, M.; Lindroos, T.; Aalto, S.; Jarvinen, E.; Karna, T.; Meinander, T. Dynamic compression testing of a tunable spring element consisting of a magnetorheological elastomer. *Smart Mater. Struct.* **2007**, *16*, 506.
- (8) Zhang, W.; Gong, X. L.; Chen, L. A gaussian distribution model of anisotropic magnetorheological elastomers. *J. Magn. Magn. Mater.* **2010**, *322*, 3797.

- (9) Zhang, W.; Gong, X. L.; Xuan, S. H.; Jiang, W. Q. Temperature-dependent mechanical properties and model of magnetorheological elastomers. *Ind. Eng. Chem. Res.* **2011**, *50*, 6704.
- (10) Jolly, M. R.; Carlson, J. D.; Munoz, B. C.; Bullions, T. A. The magnetoviscoelastic response of elastomer composites consisting of ferrous particles embedded in a polymer matrix. *J. Intell. Mater. Syst. Struct.* **1996**, *7*, 613.
- (11) Chen, L.; Gong, X. L.; Jiang, W. Q.; Yao, J. J.; Deng, H. X.; Li, W. H. Investigation on magnetorheological elastomers based on natural rubber. *J. Mater. Sci.* **2007**, *42*, 5483.
- (12) Li, J. F.; Gong, X. L.; Xu, Z. B.; Jiang, W. Q. The effect of pre-structure process on magnetorheological elastomer performance. *Int. J. Mater. Res.* **2008**, *99*, 1358.
- (13) Lokander, M.; Stenberg, B. Performance of isotropic magnetorheological rubber materials. *Polym. Test.* **2003**, *22*, 245.
- (14) Kim, Y. K.; Koo, J. H.; Kim, K. S.; Kim, S. H. Suppressing harmonic vibrations of a miniature cryogenic cooler using an adaptive tunable vibration absorber based on magneto-rheological elastomers. *Rev. Sci. Instrum.* **2011**, *82*,
- (15) Opie, S.; Yim, W. Design and control of a real-time variable modulus vibration isolator. *J. Intell. Mater. Syst. Struct.* **2011**, *22*, 113.
- (16) Collette, C.; Kroll, G.; Saive, G.; Guillemier, V.; Avraam, M.; Preumont, A. Isolation and damping properties of magnetorheologic elastomers. *J. Phys.: Conf. Ser.* **2009**, *149*, No. 012091.
- (17) Li, W. H.; Kostidis, K.; Zhang, X. Z.; Zhou, Y. Development of a force sensor working with MR elastomers. *2009 IEEE/ASME International Conference on Advanced Intelligent Mechatronics (AIM)*; IEEE: Piscataway, NJ, 2009; p 233.
- (18) Wang, X. J.; Gordaninejad, F.; Calgar, M.; Liu, Y. M.; Sutrisno, J.; Fuchs, A. Sensing behavior of magnetorheological elastomers. *J. Mech. Des.* **2009**, *131*, No. 091004.
- (19) Wang, X. J.; Gordaninejad, F.; Calgar, M.; Liu, Y. M.; Sutrisno, J.; Fuchs, A. Electrical properties of magneto-rheological elastomers. *Smasis2008: Proceedings of the ASME Conference on Smart Materials, Adaptive Structures and Intelligent Systems*; American Society of Mechanical Engineers: New York, 2009; Vol. 1, p 869.
- (20) Tian, T. F.; Li, W. H.; Deng, Y. M. Sensing capabilities of graphite based MR elastomers. *Smart Mater. Struct.* **2011**, *20*, No. 025022.
- (21) Farshad, M.; Le Roux, M. Compression properties of magnetostrictive polymer composite gels. *Polym. Test* **2005**, *24*, 163.
- (22) Mouritz, A. P.; Gardiner, C. P. Compression properties of fire-damaged polymer sandwich composites. *Composites, Part A: Appl. Sci. Manuf.* **2002**, *33*, 609.
- (23) Koo, J. H.; Khan, F.; Jang, D. D.; Jung, H. J. Dynamic characterization and modeling of magneto-rheological elastomers under compressive loadings. *J. Phys.: Conf. Ser.* **2009**, *149*, No. 012093.
- (24) Bica, I. Compressibility modulus and principal deformations in magneto-rheological elastomer: The effect of the magnetic field. *J. Ind. Eng. Chem.* **2009**, *15*, 773.
- (25) Guan, X. C.; Dong, X. F.; Ou, J. P. Magnetostrictive effect of magnetorheological elastomer. *J. Magn. Magn. Mater.* **2008**, 158.
- (26) Ginder, J. M.; Clark, S. M.; Schlotter, W. F.; Nichols, M. E. Magnetostrictive phenomena in magnetorheological elastomers. *Int. J. Mod. Phys. B* **2002**, *16*, 2412.
- (27) Coquelle, E.; Bossis, G. Magnetostriction and piezoresistivity in elastomers filled with magnetic particles. *J. Adv. Sci.* **2005**, *17*, 132.
- (28) Claeysen, F.; Lhermet, N.; LeLetty, R.; Bouchilloux, P. Actuators, transducers and motors based on giant magnetostrictive materials. *J. Alloys Compd.* **1997**, *258*, 61.
- (29) Anjanappa, M.; Wu, Y. F. Magnetostrictive particulate actuators: Configuration, modeling and characterization. *Smart Mater. Struct.* **1997**, *6*, 393.
- (30) Fuchs, A.; Zhang, Q.; Elkins, J.; Gordaninejad, F.; Evrensel, C. Development and characterization of magnetorheological elastomers. *J. Appl. Polym. Sci.* **2007**, *105*, 2497.
- (31) Chen, L.; Gong, X. L.; Li, W. H. Microstructures and viscoelastic properties of anisotropic magnetorheological elastomers. *Smart Mater. Struct.* **2007**, *16*, 2645.
- (32) Gong, X. L.; Zhang, X. Z.; Zhang, P. Q. Fabrication and characterization of isotropic magnetorheological elastomers. *Polym. Test.* **2005**, *24*, 669.
- (33) Bose, H. Viscoelastic properties of silicone-based magnetorheological elastomers. *Int. J. Mod. Phys. B* **2007**, *21*, 4790.
- (34) Wang, Y. L.; Hu, Y.; Gong, X. L.; Jiang, W. Q.; Zhang, P. Q.; Chen, Z. Y. Preparation and properties of magnetorheological elastomers based on silicon rubber/polystyrene blend matrix. *J. Appl. Polym. Sci.* **2007**, *103*, 3143.
- (35) Coquelle, E.; Bossis, G. Mullins effect in elastomers filled with particles aligned by a magnetic field. *Int. J. Solids Struct.* **2006**, *43*, 7659.